CHIN. PHYS. LETT. Vol. 32, No. 4 (2015) 047501

Doping Effect of Co at Ag Sites in Antiperovskite Mn_3AgN Compounds *

CHU Li-Hua(褚立华)[1,2], WANG Cong(王聪)[2**], SUN Ying(孙莹)[2], LI Mei-Cheng(李美成)[1], WAN Zi-Pei(万子裴)[1], WANG Yu(王宇)[1], DOU Shang-Yi(窦尚轶)[1], CHU Yue(楚月)[1]

[1]*State Key Laboratory of Alternate Electrical Power System with Renewable Energy Sources, School of Renewable Energy, North China Electric Power University, Beijing 102206*

[2]*Center for Condensed Matter and Materials Physics, Department of Physics, Beihang University, Beijing 100191*

(Received 8 December 2014)

Antiperovskite compounds $Mn_3Ag_{1-x}Co_xN$ ($x = 0.2$, 0.5 and 0.8) are synthesized and the doping effect of the magnetic element Co at the Ag site is investigated. The crystal structure is not changed by the introduction of Co. However, with the increase of the content of Co, the spin reorientation gradually disappears and the antiferromagnetic transition changes to the ferromagnetic transition at the elevated temperature when $x = 0.8$. In addition, all of the magnetic phase transitions at the elevated temperature are always accompanied by the abnormal thermal expansion behaviors and an entropy change. Moreover, when $x = 0.8$, the coefficient of linear expansion is $-1.89 \times 10^{-6}\,K^{-1}$ (290–310 K, $\Delta T = 20\,K$), which is generally considered as the low thermal expansion.

PACS: 75.50.Ee, 75.50.Gg, 65.40.De DOI: 10.1088/0256-307X/32/4/047501

Mn-based antiperovskite Mn_3AX (A= Zn, Cu, Ag, Ni etc. X= N, C etc.) series with cubic structure and $Pm3m$ space group symmetry have attracted considerable attention due to their interesting physical properties derived from the relationship between magnetic properties and crystal lattices, such as magnetocaloric effect,[1] giant magnetoresistance,[2] abnormal thermal expansion,[3–5] giant magnetostriction,[6,7] and shape memory effects.[8] In addition, these compounds have a number of advantages, e.g. they are stable in air, have good mechanical properties,[9–12] and high electric and thermal conductivity.[13]

In these compounds, the magnetic Mn metallic atoms are located at the face-centered positions in a cubic lattice; the A atom lies at the cubic corner and the nonmetallic X atom occupies the body-centered position. Antiperovskite manganese nitrides are strongly electron-correlated materials. In Mn_3AX, narrow bands are formed near the Fermi level by the strong hybridization between X 2p and Mn 3d orbitals. The occupation of these narrow bands is changed sensitively with the number of the valence electrons on the A site due to the fact that the A atoms provide the itinerant electrons at the Fermi level. Hence, the element A plays an essential role since it contributes directly to the electronic states near the Fermi level that exert a dominant effect on the physical properties.

In this work, the antiperovskite $Mn_3Ag_{1-x}Co_xN$ ($x = 0.2$, 0.5 and 0.8) compounds were successfully synthesized and the doping effect of the magnetic element Co at Ag sites on the physical properties of antiperovskite Mn_3AgN compounds was investigated by means of magnetic, lattice and specific heat measurements. The results show that the spin reorientation gradually disappears with the increase of the content of Co. Moreover, the antiferromagnetic transition becomes ferrimagnetic at an elevated temperature when $x = 0.8$ accompanied by the negative thermal expansion behaviors and an entropy change.

Polycrystalline samples with nominal compositions of $Mn_3Co_{1-x}Ag_xN$ ($0 \leq x \leq 1$) were prepared by a solid-state reaction in a vacuum (10^{-5} Pa) by using Mn_2N, Co (99.99%), and Ag (99.99%) as starting materials. Initially, the binary precursor Mn_2N was prepared by firing Mn powder (99.99%) in nitrogen gas at 750℃ for 60 h. The stoichiometric amounts of the precursors corresponding to the desired x values of 0.2, 0.5, 0.8 were mixed together, milled and pressed into a pellet by using a hydraulic press. The pellets were wrapped in a tantalum foil, sealed in vacuum in a quartz tube, sintered at 800℃ for 80 h, and then cooled to room temperature. The procedure was repeated until a pure single phase was obtained.

The crystallinity and phase of the obtained samples were studied by using powder x-ray diffraction (PANalytical X'Pert Pro multipurpose XRD) analysis performed at room temperature by using monochromatic Cu K_α radiation in the 2θ range 20°–110°. Then the lattice parameters were determined by the Rietveld analysis, which was performed by using the Fullprof program. For the lattice variation with temperature, i.e., thermal expansion properties, variable temperature x-ray diffraction ranging from 220 to

*Supported by the National Natural Science Foundation of China under Grant No 51172012, and the Fundamental Research Funds for the Central Universities.

**Corresponding author. Email: congwang@buaa.edu.cn

360 K was carried out on an X'Pert PRO powder diffractometer. The sample was heated to the desired temperature at a rate of 10 K/min and kept for 10 min for the XRD measurement. The XRD patterns at different temperatures were recorded, and then the lattice parameters were determined by the Powder X software.[14] The temperature dependence of magnetic susceptibility was measured between 5 K and 350 K in an applied magnetic field of 30 kOe, by using the quantum design magnetic property measurement system (Quantum Design MPMS-XL). The measurements were conducted under both zero-field-cooling (ZFC) and field cooling (FC) conditions by using a specific quantity of loosely gathered powder of each compound.

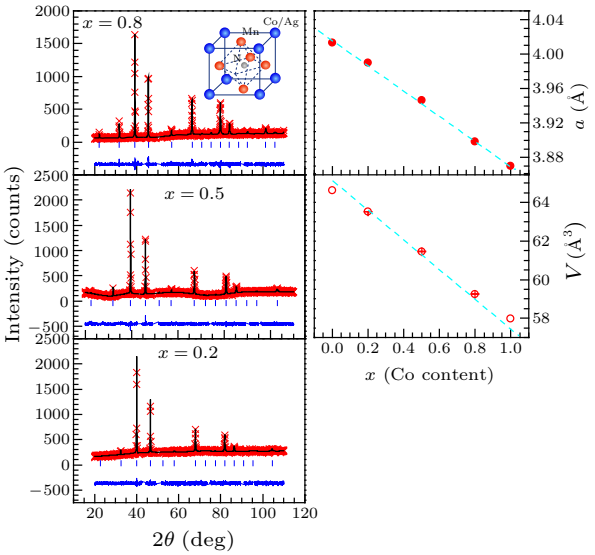

Fig. 1. (Left) Rietveld analysis of the XRD patterns for $Mn_3Ag_{1-x}Co_xN$ observed at room temperature. The cross marks and solid lines show the observed and calculated patterns, respectively. The difference between them is shown at the bottom of each panel. The positions of the Bragg reflections are marked by ticks. Excluded regions are the diffraction peaks of copper. The plot in the inset shows the schematic crystal structure of $Mn_3Ag_{1-x}Co_xN$. (Right) Variations of the cubic lattice parameter and lattice volume versus x (Co content). The error bars are smaller than the data markers.

The crystal structures of the $Mn_3Ag_{1-x}Co_xN$ (x = 0.2, 0.5 and 0.8) compounds were analyzed by XRD using the Fullprof software. Figure 1 shows the XRD patterns for the $Mn_3Ag_{1-x}Co_xN$ compounds observed at ambient temperature and pressure. An initial analysis of all the patterns was carried out by assuming a $Pm3m$ unit cell with N, Ag/Co, and Mn atoms at the 1a site (0, 0, 0), 1b site (1/2, 1/2, 1/2), and 3d site (1/2, 0, 0), respectively. As a result, all the diffraction peaks could be fitted well with this model, indicating that the $Pm3m$ model is suitable for $Mn_3Ag_{1-x}Co_xN$ compounds. It is worth noting that peaks related to impurities were not noticeable in any of the patterns, indicating the excellent quality of the compounds prepared.

The cubic lattice constant was calculated by the analysis of the XRD patterns and is displayed on the right of Fig. 1 along with the cubic unit cell volume as a function of the cobalt concentration. The data of Mn_3AgN and Mn_3CoN were previously measured by our group[15] (the work about Mn_3CoN is submitted). The lattice constant decreases linearly with the increase of the cobalt content, which is due to the fact that the atomic radius of silver is larger than that of cobalt. The plot also indicates that cobalt does indeed replace silver in the cubic structure as designed.

Most of the interesting changes in the physical properties of antiperovskite compounds are caused by the magnetic phase transition, thus we investigate the magnetic properties of the $Mn_3Ag_{1-x}Co_xN$ compounds, as shown in Fig. 2. For each curve, a bifurcation exists between the ZFC and FC curves at low temperature, implying the appearance of the magnetic frustration.[16] When x = 0.2 and 0.5, i.e., $Mn_3Ag_{0.8}Co_{0.2}N$ and $Mn_3Ag_{0.5}Co_{0.5}N$, the magnetic transition curves $M(T)$ exhibit two cusps. The magnetic transitions at the elevated temperatures are caused by the antiferromagnetic transition. According to Fruchart *et al.* and our previous work about the $Mn_3Ni_{1-x}Ag_xN$ compounds, it can be speculated that the low-temperature magnetic transition should be ascribed to a spin reorientation,[15,17] which is often observed in the antiperovskite Mn_3XN (X=Ag, Ni, Sn, etc.) compounds.[17–19]

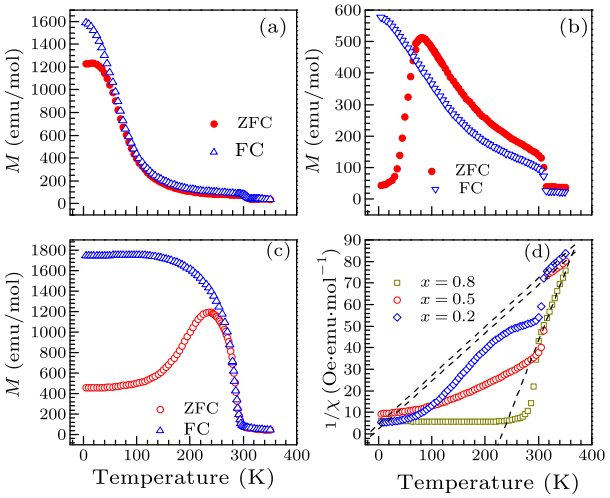

Fig. 2. Temperature dependence of the magnetization for $Mn_3Ag_{1-x}Co_xN$ compounds: (a) x = 0.2, (b) x = 0.5 and (c) x = 0.8. (d) Temperature dependence of the inverse magnetization of the $Mn_3Ag_{1-x}Co_xN$ compounds. The dashed lines correspond to a linear fit.

Fruchart *et al.* reported that the magnetic structure of Mn_3AgN below 55 K is the combination of two triangular AFM structures, i.e., Γ_{5g} and Γ_{4g}. Mn_3AgN between 55 and 290 K, an entirely triangular AFM Γ_{5g} exists. That is, the presence of trian-

gular AFM in Mn_3AgN is based on the symmetry of Γ_{4g} and Γ_{5g} or their combination of these magnetic structures, i.e., rotation of the triangular magnetic moment in the (111) crystal plane. As the temperature decreases, the rotation occurs and the axis changes with no changes in the magnitude of moments or in the lattice, and then the spin reorientation occurs. For the $Mn_3Ag_{1-x}Co_xN$ compounds, when $x = 0.2$ and 0.5, as the temperature decreases, the paramagnetic-antiferromagnetic (PM–AFM) transition occurs. With a further decrease in the temperature, the spin reorientation occurs like the Mn_3AgN. However, details of these complicated spin structures should be further investigated. With the increase of magnetic element Co content, the transition at the low temperature becomes increasingly inconspicuous, and there is just one magnetic transition at the elevated temperature when $x = 0.8$.

To further determine the essential of the magnetic transition properties at the elevated temperature, the Curie–Weiss law is used to analyze the data. The expression $\chi(T) = C/(T - \Theta_W)$, where C is the Curie constant and Θ_W is the Weiss temperature, is applied to the paramagnetic phase region as shown in Fig. 2(d). For $x = 0.2$ and 0.5, Θ_W is negative indicative of dominant AFM interactions. However, for $x = 0.8$, a positive Θ_W is obtained, suggesting that the AFM interactions are no longer dominant and the ferromagnetic phase appears in the compounds.

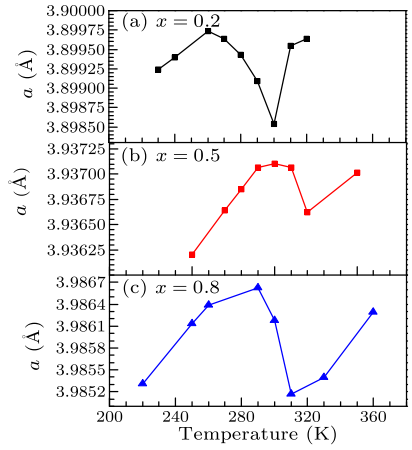

Fig. 3. Temperature dependence of the lattice parameter for $Mn_3Ag_{1-x}Co_xN$ (a) $x = 0.2$, (b) $x = 0.5$ and (c) $x = 0.8$

Antiperovskite compounds Mn_3AN are typically strongly correlated electron materials. Narrow bands are formed by the strong hybridization between N $2p$ and Mn $3d$ orbitals, whose energy levels are close to the Fermi surface, based on the Labbe'–Jardin tight binding model.[20] The A atoms provide the itinerant electrons at the Fermi level, therefore, the occupation of these narrow bands changes sensitively according to the number of valence electrons on the A site. In addition, a critical distance d_c between the Mn atoms has often been stated as being a major parameter in the characterization of the magnetic order due to the fact that the density of states at the Fermi level varies considerably at d_c. The number of valence electrons and atomic radius are different between Ag and Co, thus the occupation of these narrow bands and the critical distance will change after the substitution Co at the Ag site.[21,22]

Furthermore, the metal A can modify the intra- and (even more) the inter-atomic exchange integrals and thus contributes to the diversity of magnetic structures. Co, as a $3d$ magnetic metal element, not only is involved in the magnetic interaction through the above two methods, but also can be directly involved in the interaction between the Mn–Mn magnetic atoms to participate directly in the role for forming magnetic phases. Thus the introduction of Co in the lattice will shift the energy levels close to the Fermi surface, leading to different magnetic behaviors as a function of temperature.

Figure 3 shows the temperature dependence of the lattice constant for $Mn_3Ag_{1-x}Co_xN$. All of the $Mn_3Ag_{1-x}Co_xN$ compounds present negative thermal expansion behavior around the magnetic transition at the elevated temperature, while the cubic structure remains in the whole measured temperature range. The line coefficients of the thermal expansion are $-3.92 \times 10^{-6}\,K^{-1}$ (260–300 K, $\Delta T = 40$ K), $-4.96 \times 10^{-6}\,K^{-1}$ (300–320 K, $\Delta T = 20$ K) and $-1.89 \times 10^{-6}\,K^{-1}$ (290–310 K, $\Delta T = 20$ K), which are generally considered as the low thermal expansion (LTE), for $Mn_3Ag_{0.8}Co_{0.2}N$, $Mn_3Ag_{0.5}Co_{0.5}N$ and $Mn_3Ag_{0.2}Co_{0.8}N$, respectively. However, there is no abnormal change in the lattice around the reorientation magnetic transition when $x = 0.2$ and 0.5.

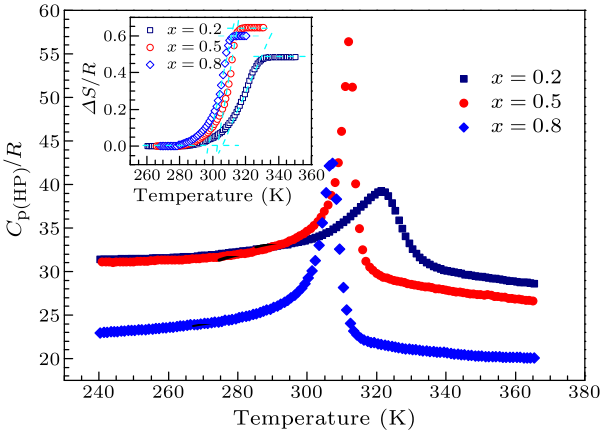

Fig. 4. Temperature dependence of the specific heat C_p of $Mn_3Ag_{1-x}Co_xN$ ($x = 0.2$, 0.5 and 0.8) compounds at the high-temperature transition. The inset shows the estimation of entropy increments S.

To further investigate the nature of the magnetic transitions, the specific heat C_p was measured over

the temperature range 240–370 K, as shown in Fig. 4. The peaks in the plot of C_p versus T are separately observed at 320 K, 310 K and 307 K for $x = 0.2$, 0.5 and 0.8, close to the high-temperature magnetic transition. To estimate the transition entropy ΔS, the polynomial function was first applied to the C_p–T data above and below the transition, excluding the region near the transition. We then subtracted the polynomial function from the total C_p and integrated the result versus temperature. This procedure results in an estimate of ΔS of approximately $0.49R$, $0.64R$ and $0.60R$ for $x = 0.2$, 0.5 and 0.8, respectively, where R is the molar gas constant. The entropy increments ΔS and the enthalpy increments ΔH are shown in Table 1.

Table 1. The entropy increments ΔS and the enthalpy increments ΔH at the transitions.

Sample	T_1 (K)	$\Delta S_1/R$	ΔH_1 (J/mol)
$Mn_3Ag_{0.8}Co_{0.2}N$	321.40	0.49	1309.34
$Mn_3Ag_{0.5}Co_{0.5}N$	311.97	0.64	1659.98
$Mn_3Ag_{0.2}Co_{0.8}N$	307.38	0.60	1533.33

The observed entropies may be ascribed to three additive contributions $\Delta S = \Delta S_l + \Delta S_m + \Delta S_e$. The contributions are caused by the volume, magnetic and electronic changes, respectively. We can estimate roughly by the relation where the thermal expansion coefficient is obtained from the variation of the lattice parameter with the temperature; κ is the isothermal compressibility estimated to be $0.5 \times 10^{-11}\,\mathrm{Pa}^{-1}$[23] and ΔV is the volume change at the transition. From this, we obtain that $\Delta S_1/R$ at the elevated temperatures for $Mn_3Ag_{0.8}Co_{0.2}N$, $Mn_3Ag_{0.5}Co_{0.5}N$ and $Mn_3Ag_{0.2}Co_{0.8}N$ are ~ -0.51, ~ -0.26 and ~ -0.31, thus $\Delta S_m + \Delta S_e \sim 1R$, $0.9R$ and $0.91R$, respectively. However, independent ΔS_m and ΔS_e cannot be obtained from the present data only. Since the measurements of heat capacity C_p are affected by the nature of the magnetic transition, additional studies are expected to make further quantitative analysis possible.

In conclusion, we have discussed the doping effect of Co on the magnetic, thermal expansion properties and heat capacity in the antiperovskite compounds $Mn_3Ag_xCo_{1-x}N$. When $x = 0.2$ and 0.5, the magnetic transition exists due to spin reorientation as the temperature decreases. As the content of Co increases, the spin reorientation gradually disappears, moreover, the antiferromagnetic transition at the elevated temperature becomes ferrimagnetic transition when $x = 0.8$. Isotropic negative thermal expansion behavior is observed around the magnetic transition at the elevated temperature in all of the samples. Especially, when $x = 0.8$, the coefficient of the linear expansion is $-1.89 \times 10^{-6}\,\mathrm{K}^{-1}$ (290–310 K, $\Delta T = 20$ K), which is generally considered as the LTE. Furthermore, all the magnetic transitions at the elevated temperature are accompanied by an entropy change, about $0.49R$, $0.64R$ and $0.60R$ for $x = 0.2$, 0.5 and 0.8, respectively.

References

[1] Hamad M A 2014 *J. Supercond. Novel Magn.* **27** 2569
[2] Kamishima K, Goto T, Nakagawa H, Miura N, Ohashi M and N Mori 2000 *Phys. Rev.* B **63** 024426
[3] Wang C, Chu L H, Yao Q R, Sun Y, Wu M M, Ding L, Yan J, Na Y Y, Tang W H, Li G N, Huang Q Z and Lynn J W 2012 *Phys. Rev.* B **85** 220103(R)
[4] Song X Y, Sun, Z H, Huang Q Z, Rettenmayr M, Liu X M, Seyring M, Li G N, Rao G H and Yin F X 2011 *Adv. Mater.* **23** 4690
[5] Tan J, Huang R J, Li W, Han Y M and Li L F 2014 *J. Alloys Compd.* **593** 103
[6] Shimizu T, Shibayama T, Asano K and Takenaka K 2012 *J. Appl. Phys.* **111** 07A903
[7] Wang B S, Tong P, Sun Y P, Li L J, Tang W, Lu W J, Zhu X B, Yang Z R and Song W H 2009 *Appl. Phys. Lett.* **95** 222509
[8] Takenaka K Hamada T, Shibayama T and Asano K 2013 *J. Alloys Compd.* **577** S291
[9] Tong P, Wang B S and Sun Y P 2013 *Chin. Phys.* B **22** 067501
[10] Nakamura Y, Takenaka K, Kishimoto A and Takagi H 2009 *J. Am. Ceram. Soc.* **92** 2999
[11] Huang R J, Wu Z X, Yang H H, Chen Z, Chu X X and Li L F 2010 *Cryogenics* **50** 750
[12] Hu J Y, Wen Y C, Yao Y, Wang C, Zhan Q, Jin C Q and Yu R C 2012 *Chin. Phys. Lett.* **29** 086201
[13] Takenaka K and Takagi H 2006 *Mater. Trans.* **47** 471
[14] Cheng D 1999 *J. Appl. Crystallogr.* **32** 838
[15] Chu L H, Wang C, Yan J, Na Y Y, Ding L, Sun Y and Wen Y C 2012 *Scr. Mater.* **67** 173
[16] Lin S, Wang B S, Lin J C, Zhang L, Hu X B, Huang Y N, Lu W J, Zhao B C, Tong P, Song W H and Sun Y P 2011 *Appl. Phys. Lett.* **99** 172503
[17] Fruchart D and Bertaut E F 1978 *J. Phys. Soc. Jpn.* **44** 781
[18] Gomonaj E V 1989 *Phase Transit.* **18** 93
[19] Gomonaj E V and L'Vov V A 1992 *Phase Transit.* **40** 225
[20] Jardin J P and LabbéJ 1975 *J. Phys. France* **36** 1317
[21] Gerasimov E G, Gaviko V S, Neverov V N and Korolyov A V 2002 *J. Alloys Compd.* **343** 14
[22] Sun Y, Guo Y F, Tsujimoto Y, Yang J J, Shen B, Yi W, Matsushita Y, Wang C, Wang X, Li Jun, Sathish I C and Yamaura K 2013 *Inorg. Chem.* **52** 800
[23] García J et al 1980 *J. Magn. Magn. Mater.* **15** 1155